STRUCTURE OF WAVE FUNCTIONS ON THE TORUS CHARACTERIZED BY A TOPOLOGICAL CHERN INDEX

F. Faure

Institut des Sciences Nucléaires,

39026 Grenoble, France,

and

P. Lebœuf

Division de Physique Théorique[1],

Institut de Physique Nucléaire,

91406 Orsay Cedex, France.

IPNO/TH 92-93

Octobre 1992

Paper contributed to the Proceedings of the Workshop "From Classical to Quantum Chaos", G. F. Dell'Antonio, S. Fantoni and V. R. Manfredi, editors, Trieste, 21-24 July 1992.

[1]Unité de Recherche des Universités Paris XI et Paris VI associée au CNRS.

Structure of wave functions on the torus characterized by a topological Chern index

F. Faure[1] and P. Lebœuf[2]
1-Institut des Sciences Nucléaires, 38026 Grenoble, France.
2-Division de Physique Théorique, Institut de Physique Nucléaire, 91406 Orsay Cedex, France.

Abstract

We study the quantum eigenstates and eigenvalues on a toroidal two dimensional phase-space. To each eigenfunction is associated an integer, the Chern index, which tests the localization of the eigenfunction as some periodicity conditions are changed. The Chern index is a topological invariant which can only change when a spectral degeneracy occurs. We compute these topological numbers for three different models: two having an underlying regular dynamics, the third-one having a chaotic dynamics. We discuss the role played by the separatrix-states, the effects of quantum tunneling (symmetry effects) and of a classically chaotic dynamics in the spectrum of the Chern indices. The values taken by those indices are interpreted in terms of a phase-space distribution function.

I) Introduction.

In 1980, K. von Klitzing *et al* showed the remarkable result about the (integer) quantization of the Hall conductivity σ_{xy} for 2D electrons. In the following years, several explanations of this effect were proposed. In particular, using a single-particle model of electrons in a periodic potential $V(x,y)$ (the crystal lattice) and subjected to a transverse magnetic field, Thouless *et al* [1] demonstrated that σ_{xy} is quantized in integer multiples of e^2/h whenever the Fermi level lies in a spectral gap. Their explanation is topological in nature, since they related the averaged Kubo-formula for the conductivity to a Chern index, which is invariant under perturbations.

For high magnetic fields, the coupling between the different Landau levels can be neglected (Lowest Landau Level approximation) and the electron's motion is described by an effective one-dimensional hamiltonian $H(p,q)$ periodic in position as well as in momentum. For example, if $V(x,y) = \cos(2\pi x) + \alpha\cos(2\pi y)$, then the effective Hamiltonian is $H(p,q) = \cos(2\pi p) + \alpha\cos(2\pi q)$ (Harper's hamiltonian). Working in this approximation, Arovas *et al* [2] provided an interpretation of the values of the Hall conductivity in terms of the localization properties of the eigenstates. Since the system is periodic in both directions p and q, it happens that in the process of quantization two quantal parameters (θ_1, θ_2) can be introduced, related to the periodicity of the wave function under translations by an elementary cell. In agreement with the Thouless interpretation of localization [3], they found that current-carrying states are highly sensitive to changes of the boundary conditions.

From a dynamical point of view the LLL dynamics is integrable, since it corresponds to a one-dimensional motion and the energy is conserved. For lower magnetic fields we expect the electron's motion to obey chaotic solutions. An effective way to include the chaoticity into the electron's dynamics and at the same time remain in a doubly-periodic two-dimensional phase space is to consider *maps* instead of hamiltonians. The map can be considered as a Poincaré surface of section of the full electron's dynamics taking place on a four-dimensional phase space. In Ref.[4] it was shown how Chern indices can be adapted to maps in order to study the structure of eigenstates in the fully chaotic regime as well as the quantum-mechanical transition when the underlying classical dynamics changes from integrable to chaotic.

The quantization of chaotic maps offers the opportunity to analyze the quantum mechanics of a classically chaotic motion while minimizing the mathematical complexities. The purpose of this paper is to study the behaviour of eigenvalues and eigenstates of classically integrable and chaotic systems under changes of the boundary conditions (θ_1, θ_2), following the approach of Ref.[4]. For this purpose, we will combine two different objects: the Chern indices and the Husimi functions. The Chern index characterizes the sensitivity of eigenfunctions to changes of the boundary conditions. A zero Chern index means weak dependence (no sensitivity), and we said that the wave function is localized. On the contrary, when the Chern index is different from zero then the wave function is delocalized. Wave functions of quantized fully chaotic maps were found to have (generically) a non-zero Chern index [4].

On the other hand, the Husimi function, which provides a phase-space representation of quantum states, complements the information provided by the Chern index. This is because i) it can often be directly compared with classical distributions in phase space and ii) it allows a direct phase-space visualization of the modifications induced on an eigenstate by changes of the boundary conditions.

In sections II, III and IV we briefly introduce the quantum mechanics associated to a two-dimensional toroidal phase space, the coherent-state representation (which allows to introduce the Husimi function) and the definition of the Chern index with some of its properties, respectively. Then we consider integrable systems. In this case, for trajectories which don't turn around the toroidal phase space (i.e. trajectories contractible to a point), W.K.B. theory gives a semi-classical expression for the eigenfunctions with an exponentially small sensitivity to changes of (θ_1, θ_2). The quantum particle remains, for arbitrary boundary conditions, exponentially localized around the quantized classical trajectory. This implies the vanishing of the Chern index for those states [4]. In section V, we will consider a model in which the state having a non zero Chern index is associated to a non contractible separatrix, whose energy changes as a parameter is varied.

However, we find in general that even for integrable systems the Chern indices are not zero whenever the quantized hamiltonian is invariant under "smaller" translations $\hat{T}_Q^{n/m}$, $\hat{T}_P^{n'/m'}$, with integers $n, n' < m, m'$ (for example, the hamiltonian $H(p,q) = \cos(4\pi p) + \alpha\cos(2\pi q)$ is invariant under $\hat{T}_P^{1/2}$. See below the definition of the operators $\hat{T}_Q$ and $\hat{T}_P$). Contrarily to the preceding case, due to a resonance effect between degenerate trajectories (related to tunneling) the Chern index is non-zero for all the eigenstates. In section VI we study, in a model with three wells,

how this resonance effect disappears as the "smaller" symmetry is broken.

Finally, in section VII we also study some consequences of the existence of "smaller" symmetries on quantized chaotic maps. These topics are treated briefly. More extensive analytical as well as numerical results will be published elsewhere [5].

II) Quantum mechanics on the torus.

We consider a one-degree-of-freedom Hamiltonian on the plane, periodic with period Q in position and P in momentum

$$H(q,p) = H(q+Q,p) = H(q,p+P). \tag{1}$$

By identifying all the domains of sides (Q,P), the classical mechanics can be restricted to a torus. Quantum mechanically, Eq.(1) reads

$$[\hat{T}_Q, \hat{H}] = [\hat{T}_P, \hat{H}] = 0, \tag{2}$$

where $(\hat{T}_Q, \hat{T}_P)$ are the translations operators in position and momentum, respectively

$$\hat{T}_Q = e^{-iQ\hat{p}/\hbar} \qquad\qquad \hat{T}_P = e^{iP\hat{q}/\hbar}.$$

The three operators $\hat{H}, \hat{T}_Q, \hat{T}_P$ commute if in addition $[\hat{T}_Q, \hat{T}_P] = 0$, which is equivalent to $QP = Nh$ with $N \in \mathbb{N}$. The latter equation, which we henceforth assume to be true, has a geometrical interpretation: the total volume of the classical phase space must be an integer multiple of Planck's constant. N is therefore interpreted as the number of quantum states in Hilbert space. Such a relation, which holds exactly in the case of a toroidal geometry, generally occurs when we deal with quantum mechanics on a compact phase space and is reminiscent of the Weyl or Thomas-Fermi semiclassical approximation of the number of states up to energy E. Correspondingly, the classical limit is obtained when $N \to +\infty$.

A state $|\Psi>$ is an eigenvector of the unitary operator $\hat{T}_Q$ and $\hat{T}_P$ if:

$$\begin{cases} \hat{T}_Q|\Psi> = e^{i\theta_1}|\Psi> \\ \hat{T}_P|\Psi> = e^{i\theta_2}|\Psi> . \end{cases} \tag{3}$$

In this way, a couple of parameters $(\theta_1, \theta_2) \in [0; 2\pi]^2$ characterizes the N-dimensional Hilbert space $\mathcal{H}_N(\theta_1, \theta_2)$. Equations (2) guarantee the invariance of that space under the time evolution. Therefore for a given classical dynamics on the torus with hamiltonian $H(p,q)$, there are several quantum dynamics, one for each $(\theta_1, \theta_2) \in [0; 2\pi]^2$ acting on the Hilbert space $\mathcal{H}_N(\theta_1, \theta_2)$. The stationary Schrödinger equation in $\mathcal{H}_N(\theta_1, \theta_2)$ can be written

$$\hat{H}|\Psi_n(\theta_1,\theta_2)> = E_n(\theta_1,\theta_2)|\Psi_n(\theta_1,\theta_2)> \qquad\qquad n = 1 \to N.$$

In the case of maps, quantum-mechanically the system is defined by a one-step evolution operator $\hat{U}$. The eigenvalue problem now takes the form

$$\hat{U}|\Psi_n(\theta_1,\theta_2)> = e^{-iE_n(\theta_1,\theta_2)}|\Psi_n(\theta_1,\theta_2)> \qquad\qquad n = 1 \to N, \tag{4}$$

where $E_n \in [-\pi;\pi]$ is the quasi-energy.

III) Coherent-state representation.

A coherent state $|qp>$ of the plane is a gaussian wave packet with mean-values: $<\hat{q}>=q, \quad <\hat{p}>=p, \quad \Delta q\Delta p=\hbar/2 \qquad (<.>\equiv<qp|.|qp>)$, given by [6, 7]:

$$|qp>=|z>=e^{\bar{z}a^+}|0> \qquad z=\frac{1}{\sqrt{2}}(q-ip).$$

The family of all coherent states $|z>$ forms an over-complete basis and defines the Fock-Bargmann representation of a state $|\Psi>$:

$$\psi(z)=<z|\Psi> \qquad : \text{analytic function of } z.$$

For a state $|\Psi>\in \mathcal{H}_N(\theta_1,\theta_2)$, $\psi(z)$ is a Jacobi theta-function with exactly N zeros $((z_k(\theta_1,\theta_2))_{k=1\to N})$ on the torus [8]. The Husimi distribution of the state $|\Psi>$ represents a quasi-probability density on the phase space (it is not a probability density because coherent states are not orthogonal, but they tend to be so in the classical limit):

$$W_\Psi(q,p)=\frac{|<qp|\Psi>|^2}{<qp|qp>}.$$

IV) The Chern index.

When (θ_1,θ_2) are varied, $E_n(\theta_1,\theta_2)$ defines a band, and $|\Psi_n(\theta_1,\theta_2)>$ defines a surface in the space of states - the canonical complex line bundle with a $U(1)$ fiber corresponding to the phase [9] - whose topology can be characterized by an integer, the Chern index, provided no degeneracy occurs [9, 10]:

$$C_n=\frac{i}{2\pi}\iint d\theta_1 d\theta_2\,(<\partial_{\theta_1}\Psi_n|\partial_{\theta_2}\Psi_n>-<\partial_{\theta_2}\Psi|\partial_{\theta_1}\Psi_n>), \qquad n=1\to N. \qquad (5)$$

An interpretation of the Chern index in terms of the behaviour of its associated Husimi function is the following: if there is a point (q_0,p_0) in phase space for which $W_{\Psi_n(\theta_1,\theta_2)}(q_0,p_0)$ is never zero when the parameters (θ_1,θ_2) are varied, then $C_n=0$. We say in this case that the wave function is localized (in phase space; in fact, the same argument can be employed in any other representation). Thus eigenstates of quantized classically integrable systems, whose Husimi distribution is localized on a contractible trajectory, will generically have zero Chern index. In general, the Chern index counts the algebraic number of times the zeros of the wave function cover each point z_1 of the phase space ($+1$ or -1 according to the orientation of the mapping $z_k(\theta_1,\theta_2)$, and the result doesn't depend on the point z_1 chosen) [11, 2].

The Chern index of a given quantum state $|\Psi_n>$ can only change when a spectral degeneracy between bands occur. For a conical intersection, the Chern index changes by ± 1. For

a one-parameter hamiltonian $\hat{H}(\gamma)$, level-crossings can only happen at isolated points of the parameter space $(\theta_1, \theta_2, \gamma)$. But the sum of the Chern numbers of the (generically two) touching bands is conserved [10]. This implies that the total sum of the Chern indices is conserved, and can be shown to be one $\sum_{n=1}^{N} C_n = 1$. Away from degeneracies, the Chern index of each band remains constant. In the quantum Hall effect, C_n measures the conductivity of the band when a weak electric field is applied to the system (the linear response approximation) [1]. In this context, a non zero Chern index (delocalized state) is synonymous of a conducting state.

V) Separatrix and delocalized states.

As we said before, for an integrable dynamics eigenstates associated with trajectories contractible to a point will have generically a zero Chern index. We say generically because in the next section we will see an example where, due to an additional symmetry, trajectories are in resonance, and all quantum states have a non-zero Chern index. Furthermore, $\sum_{n=1}^{N} C_n = 1$. This means that if for example we take the Harper model, whose phase-space energy curves are shown in Fig.1, then only the quantum states associated with the separatrix (which is not contractible to a point) is expected to have $C_n = 1$ and therefore to be delocalized. For odd N, only one state will be associated to the separatrix.

In order to stress this association between a non-contractible separatrix and a non-zero Chern index, we now consider a modified Harper hamiltonian depending on a parameter $D \in [0; 1]$, in order to move up the energy of the classical separatrix and force the Chern index equal to one to pass from one eigenstate to another with higher energy. This "hopping" of the Chern index can only happen through spectral degeneracies between the bands.

The Harper-like hamiltonian is:

$$H(p, q) = -\cos(2\pi q) - \cos(2\pi p) - D\cos(2\pi(q - p)). \tag{6}$$

Figure 2 shows some energy bands and their associated Chern indices for $N = 21$ as a function of D. Each band is represented by two lines, its upper and lower values in (θ_1, θ_2)-space. To be able to identify neighbouring bands, we have alternated between continuous and dashed-lines to represent them. Degeneracies between neighbouring bands are indicated by a short vertical segment joining the degenerate bands. The values for the Chern indices indicated in the Figure hold for each band in the whole D-interval between degeneracies. When not explicitly indicated, it must be assumed that $C_n = 0$.

Our first observation is that, for all energies, there is always a state that follows the non-contractible separatrix, whose energy is represented by a dashed-line going upwards in energy as a function of D. This is done through a series of degeneracies between neighbouring bands. In this way, the energy of the state having $C = 1$ increases, and closely following the classical energy curve of the separatrix. The second separatrix, appearing at $D = 0.5$ and represented by a dashed line going downwards in energy in Fig.2, is contractible to a point and does not support a state with $C \neq 0$ (cf section VII). Secondly, the bands with $C_n = 0$ are associated

with quantized trajectories contractible to a point. The narrowness of these bands, far away from the separatrix, is explained by the fact that in this case the WKB expression for the energy has an exponentially small dependence on (θ_1, θ_2) [12].

In Figure 3 we plot the Husimi function of the delocalized state Ψ_{13} ($C_{13} = 1$) for $D = 0.5$, $N = 21$ and for several values of (θ_1, θ_2). The plot uses a grey scale, with higher (lower) intensities in black (white). The small stars indicate the position of the 21 zeros of that state. As the parameters (θ_1, θ_2) are varied, a zero passes through *each* point of phase space *once* [2] (see Figure 4).

VI) A three-well hamiltonian.

In the previous model, only the separatrix was responsible for a non-zero Chern index. We now consider an integrable model in which *all* the Chern indices are non-zero. This behaviour is related to a resonant effect between different degenerate classical trajectories. A discussion of this resonant effect as well as a computation of the Chern indices can also be found in [1].

The following Hamiltonian has, for $V = 0$, three wells with a $\hat{T}_P^{1/3}$ symmetry

$$H(q,p) = -\cos(2\pi q) - \cos(6\pi p) - V\cos(8\pi p + \frac{\pi}{6}) - \frac{1}{4}\cos(2\pi q + \frac{\pi}{4}). \qquad (7)$$

The classical phase-space trajectories are shown in Fig.5. A simple semiclassical analysis (neglecting tunneling effects) fails in this case because it would give three degenerate bands. In fact, there is an exponentially small splitting between them (as in the ordinary tunnelling effect between two symmetric wells), and the eigenfunction of each band can have (depending on the value of (θ_1, θ_2)) a non-zero amplitude in each of the three wells. Because the three wells are symmetric under translation, the tunneling effect creates a non-contractible loop joining the three wells in the p direction, and this creates a strong dependence of each band on (θ_1, θ_2). This dependence makes the Husimi distribution of a given band to oscillate between the three wells as a function of (θ_1, θ_2), thus producing a non-zero Chern index.

The energy bands and the Chern indices are shown in Fig.6 for $N = 11$ as a function of V (see the caption of Figure 2). We restrict our discussion to the states $\Psi_9, \Psi_{10}, \Psi_{11}$ (Fig.6b), corresponding to states located in the three wells in the center of the phase space. When $V = 0$, we observe non-zero Chern indices (whose value has been analytically expressed by Thouless et al. [1] and are given, for $N = 11$, by $-1, 2, -1, -1, 2, -1, 2, -1, -1, 2, -1$ for $n = 1, \cdots, 11$, respectively). As θ_1 is varied, the states $\Psi_9, \Psi_{10}, \Psi_{11}$ oscillate between the three wells, in correspondence with the value of the Chern index (see Figures 7-8). In Fig.8 we show how the quantum particle in the state Ψ_{11} tunnels from one well to the other as a function of θ_1 in the Husimi representation. For a given value of θ_1 the wave function is concentrated on one of two wells. The only values of θ_1 where the amplitude is shared between two wells are around the transition lines indicated in Figure 7.

As V increases, the symmetry is broken, and the states $\Psi_9, \Psi_{10}, \Psi_{11}$ get localized in one well for arbitrary (θ_1, θ_2) (the well $1, 2, 3$, respectively) and get a zero Chern index. This behaviour is expected away from the separatrix because if there is a sufficient asymmetry between the three

wells, then WKB theory (without tunneling) gives a good approximation for the individual states and, as discussed before, the quantum state is exponentially localized on the quantized classical orbit and the Chern indices are zero. The transition between non-zero and zero Chern indices is made through two successive degeneracies (figure 6b). Figure 9 shows the Husimi density of the state Ψ_{10} as a function of (θ_1, θ_2) for a phase-space point located in the well number two. Before the first degeneracy $C_{10} = 2$, and correspondingly the density gets zero twice with the same algebraic number as (θ_1, θ_2) are varied. After the first degeneracy, $C_{10} = 1$ and the density gets zero only once. Finally, after the second degeneracy, the density is always positive.

The resonance effect observed for $V = 0$ making all the Chern indices different from zero is due to the existence of a special symmetry $\hat{T}_P^{1/3}$. As the symmetry is broken ($V \neq 0$), the effect disappears and we recover the generic situation for integrable systems in which all the states (except the separatrix states) have a zero Chern index. For an arbitrary (random) Hamiltonian on the torus, Y. Huo et al [13] have shown that statistically the Chern indices are zero except for a thin range in the middle of the spectrum (whose width tends to zero in the semiclassical limit $N \to \infty$) where the Chern indices are non-zero and are therefore responsible for the conductivity. This result is in accordance with the results obtained in the two previous models.

VII) Chaotic dynamics: the kicked Harper model

We introduce a chaotic dynamics by adding a time-dependent term to a Hamiltonian. If the perturbation is periodic in time, then in general we can integrate the classical equations of motion over one period and obtain a map of the torus onto itself. By Floquet's theorem, the unitary evolution operator that quantizes the map will have N stationary states given by Eq.(4). As before, a Chern index can be associated to each band [4]. Our purpose now is to study their behaviour when the classical motion is no longer integrable.

We consider the kicked Harper hamiltonian [4]

$$H(t) = -\cos(2\pi p) - \cos(2\pi q)K(t)$$

where $K(t) = T \sum_{n \in \mathbb{Z}} \delta(t - nT)$.

Classically, we obtain the stroboscopic map between two successive kicks by integrating the equations of motion over one period T

$$\begin{cases} x_{n+1} = x_n + \gamma \sin(2\pi y_n) \\ y_{n+1} = y_n - \gamma \sin(2\pi x_{n+1}) \end{cases} \tag{8}$$

with $\gamma = 2\pi T/QP$, $\quad x = q/Q$, $\quad y = p/P$. When γ is varied, the system undergoes a transition from a regular to a chaotic dynamics (Figure 10).

The quantum propagator is given by

$$\hat{U} = T(e^{-\frac{i}{\hbar}\int_0^T H(t)dt}) = \exp(iN\gamma\cos(2\pi\hat{x}))\exp(iN\gamma\cos(2\pi\hat{y})) \tag{9}$$

with eigenvalue problem (4). In Figure 11 we show the bands and the Chern indices for $N = 11$ as a function of γ. It must be noted that the variation of the Chern index at degeneracies is

often more than one. This is a nongeneric behaviour which is due to the symmetries of the kicked Harper model.

In Figure 11, we observe three different regimes:
- In the first one, for $\gamma \in [0; 0.16(\approx \frac{\pi}{2N})]$ the classical dynamics is mostly regular, and the Chern indices coincide with those of the unperturbed Harper model.
- In the second regime, for $\gamma \in [0.16; 0.4]$, classically the dynamics is mixed. Now the quasi-energy bands cross each-other. The Chern indices remain unchanged before and after the crossing. In fact, we find that when two quasi-energies are crossing, two degeneracies change the Chern indices of the colliding bands on a very short range of γ (this width is related to the width of the bands), except for Ψ_1, Ψ_{11} because of the symmetry of the spectrum. For example, the bands Ψ_1, Ψ_2 has two degeneracies at $\gamma = 0.194557$ and $\gamma = 0.194572$, and between them the Chern index is $C = \pm 1$. The same happens between the bands Ψ_3, Ψ_4 for $\gamma = 0.2637 \rightarrow 0.2651$. Figure 12 shows a detail of the latter crossing, and the Husimi plot of Ψ_3 for $\gamma = 0.2645$ and for several values of (θ_1, θ_2). Because of the narrowness of the γ-interval, most of these small resonances between crossing bands in the mixed regime were not detected nor indicated in the original computation of the Chern indices for the kicked Harper model in [4].

As in section VI, this effect is connected to a resonance between quantized classically invariant tori (tunneling between the two tori). Without symmetries, there would have been an exponentially small repulsion between the bands, no degeneracies and no resonance effect.
- In the third regime, for $\gamma > 0.4$, the classical dynamics is dominated by a chaotic motion. Now there are many crossings between the bands, and for sufficiently high γ, *all* the Chern indices are different from zero. The width of the bands has considerably increased if compared to the two preceding regimes.

F.F. gratefully acknowledges the hospitality of the Institut de Physique Nucléaire at Orsay during his visits.

References

[1] D. J. Thouless, M. Khomoto, M. P. Nightingale, and M. den Nijs, *Phys. Rev. Lett.* **49**, 405 (1982).

[2] D. P. Arovas, P. N. Bhatt, F. D. M. Haldane, P. B. Littlewood and R. Rammal, *Phys. Rev. Lett.* **60**, 619 (1988).

[3] D. J. Thouless, *Phys. Rep.* **13**, 93 (1974).

[4] P. Lebœuf, J. Kurchan, M. Feingold and D. P. Arovas, *Phys. Rev. Lett.* **65**, 3076 (1990); Chaos **2**, 125 (1992).

[5] F. Faure and P. Lebœuf, to be published.

[6] W. M. Zhang, D. H. Feng and R. Gilmore, *Rev. of Modern Phys.* **62**, 867 (1990).

[7] A. M. Perelomov, *Generalized coherent states and their applications* (Springer, Berlin) 1986.

[8] P. Lebœuf and A. Voros *J. Phys. A: Math. Gen.* **23**, 1765 (1990).

[9] M. Nakahara, *Geometry, topology and physics*, graduate students series in physics, Adam Hilger, Bristol and N.Y.

[10] J. E. Avron, R. Seiler and B. Simon, *Phys. Rev. Lett.* **51**, 51 (1983).

[11] M. Khomoto, *Ann. of Phys.* (N.Y.) **160** , 343 (1985).

[12] M. Wilkinson, *Proc. R. Soc. Lond.* A **391**, 305 (1984).

[13] Y. Huo and R. N. Bhatt *Phys. Rev. Lett.* **68**, 1375 (1992).

Figure 1: Phase-space energy contour-lines of the Hamiltonian (6). The separatrix is represented by a the solid line. A bifurcation and a new separatrix appears at $D = 0.5$. (a): $D = 0$ (b): $D = 0.75$.

Figure 2: Energy bands and their associated Chern indices for the spectrum of the Hamiltonian (6) for $N = 21$, in the neighbourhood of the separatrix. Each band is represented by two lines (upper and lower bound), alternatively plotted using a continuous or a dotted line. The energy of the classical separatrix is indicated by a dashed line. Vertical segments indicate the occurrence of degeneracies.

Figure 3: Hamiltonian (6). The Husimi distribution of the band Ψ_{13} with a Chern index equal to one, for $D = 0.5$ and $N = 21$, for different value of (θ_1, θ_2). The stars correspond to the zeros of the distribution. We are using a grey scale with high (low) intensity regions in black (white).
(a): $(\theta_1, \theta_2) = (\pi, \pi)$. There is large intensity on the unstable fix points.
(b): $(\theta_1, \theta_2) = (0, \pi)$. A zero is located at the unstable fix point $(q, p) = (0, 0.5)$.
(c): $(\theta_1, \theta_2) = (\pi, 0)$. A zero is located at the other unstable fix point $(q, p) = (0.5, 0)$.

Figure 4: Quasi-probability density of Ψ_{13} at the unstable fix points as a function of (θ_1, θ_2) (see caption to Figure 3). We observe that as (θ_1, θ_2) are varied, the density goes to zero once; this is because the Chern index is one [2].
(a): $(q, p) = (0.5, 0)$ (b): $(q, p) = (0, 0.5)$

Figure 5: Energy-contour lines of the Hamiltonian (7).
(a): for $V = 0$, the three wells of maximum energy are symmetric under translation by $1/3$ in the p direction.
(b): for $V = 0.2$, the symmetry is broken.

Figure 6: Bands and Chern indices for the spectrum of the hamiltonian (7) for $N = 11$.
(a) The total spectrum.
(b) Detail of the spectrum for the bands $\Psi_9, \Psi_{10}, \Psi_{11}$ near $V = 0$, showing two degeneracies (vertical lines).

Figure 7: The well number (see Fig.5) where $\Psi_9, \Psi_{10}, \Psi_{11}$ are localized as θ_1 is varied, for $V = 0$ and $N = 11$. For example, Ψ_{10} makes twice the cycle $2 \to 1 \to 3$; correspondingly, its Chern number is $C = +2$.

Figure 8: Husimi distribution of Ψ_{11} for $N = 11$, $V = 0$ for several values of (θ_1, θ_2).
(a): $\theta_1 = 5$ (b): $\theta_1 = 1$ (c): $\theta_1 = 3$

Figure 9: Probability density of the state Ψ_{10} in the well number 2 for $N = 11$ as a function (θ_1, θ_2) for several values of V.
(a)$V = 0.01$: before the first degeneracy. The Husimi function vanishes twice in the (θ_1, θ_2)-plane (the zeros are marked by stars); correspondingly, the Chern index is two.
(b)$V = 0.065$: between the two degeneracies. The Husimi function vanishes once in the (θ_1, θ_2)-plane; correspondingly, the Chern index is one.
(c) $V = 0.14$: after the degeneracies. The Husimi function is strictly positive in all the (θ_1, θ_2)-plane; correspondingly, the Chern index is zero.

Figure 10: Phase-space trajectories of the classical map (8) for:
(a):$\gamma \to 0$: integrable regime.
(b):$\gamma = 0.3$: mixed regime.
(c):$\gamma = 0.7$: chaotic regime.

Figure 11: Quasi-energy bands and Chern indices for the propagator (9) for $\gamma \in [0; 0.8]$. As before, vertical segments indicate the occurrence of degeneracies between two neighbouring bands. The spectrum is symmetric with respect to $E = 0$.

Figure 12: The resonance between Ψ_3 and Ψ_4 at $\gamma = 0.2645, N = 11$.
(a) Detail of the spectrum.
Husimi distribution of Ψ_3 for (b): $(\theta_1, \theta_2) = (0, 0)$ (c): $(\theta_1, \theta_2) = (1, 1)$ (d): $(\theta_1, \theta_2) = (\pi, \pi)$.

Figure 1

(a)

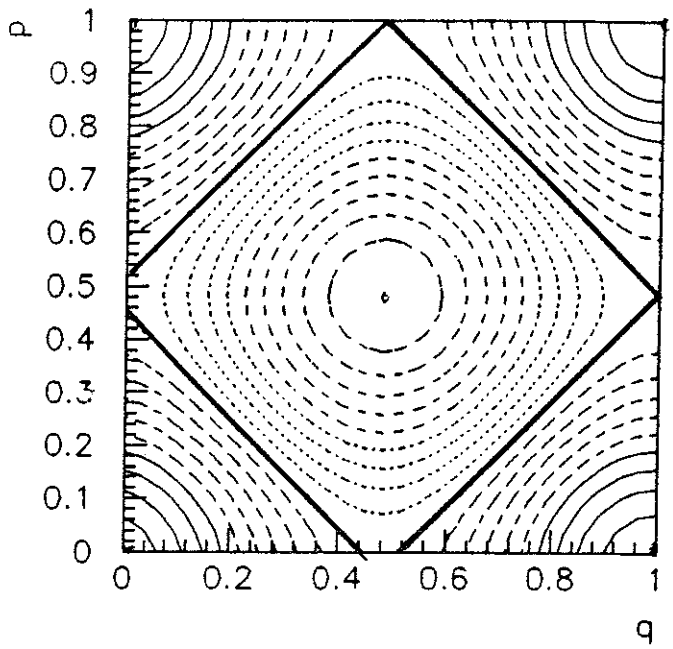
p
1
0.9
0.8
0.7
0.6
0.5
0.4
0.3
0.2
0.1
0
0
0.2
0.4
0.6
0.8
1
q

(b)

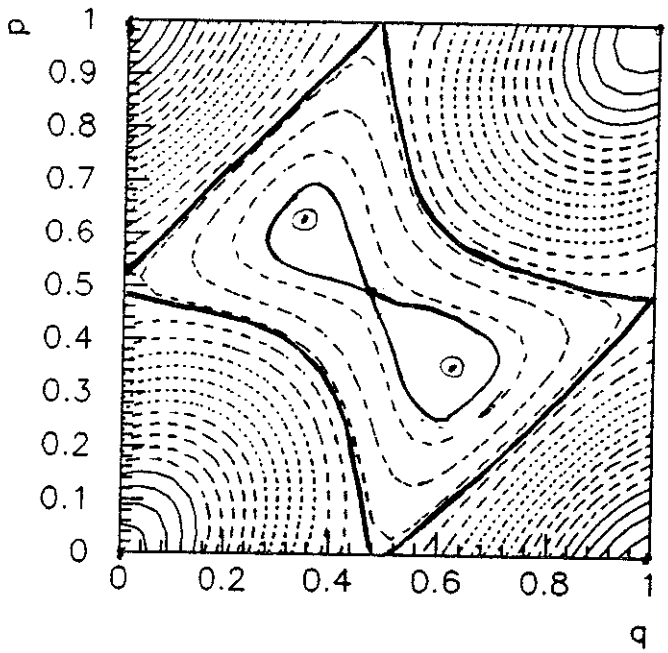
p
1
0.9
0.8
0.7
0.6
0.5
0.4
0.3
0.2
0.1
0
0
0.2
0.4
0.6
0.8
1
q

Figure 2

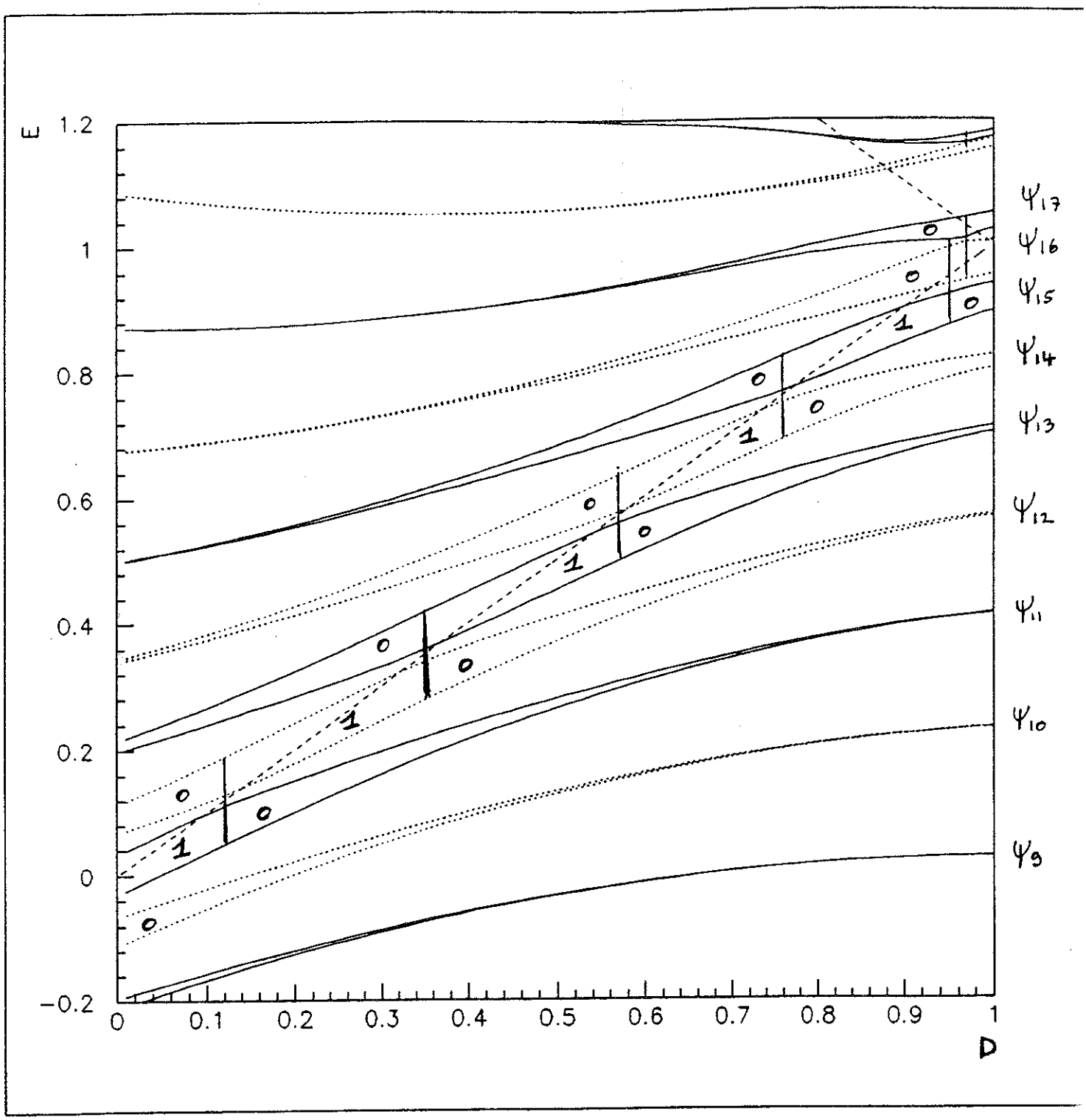
E
1.2
1
0.8
0.6
0.4
0.2
0
−0.2
0
0.1
0.2
0.3
0.4
0.5
0.6
0.7
0.8
0.9
1
D
ψ17
ψ16
ψ15
ψ14
ψ13
ψ12
ψ11
ψ10
ψ9
0
1

Figure 3

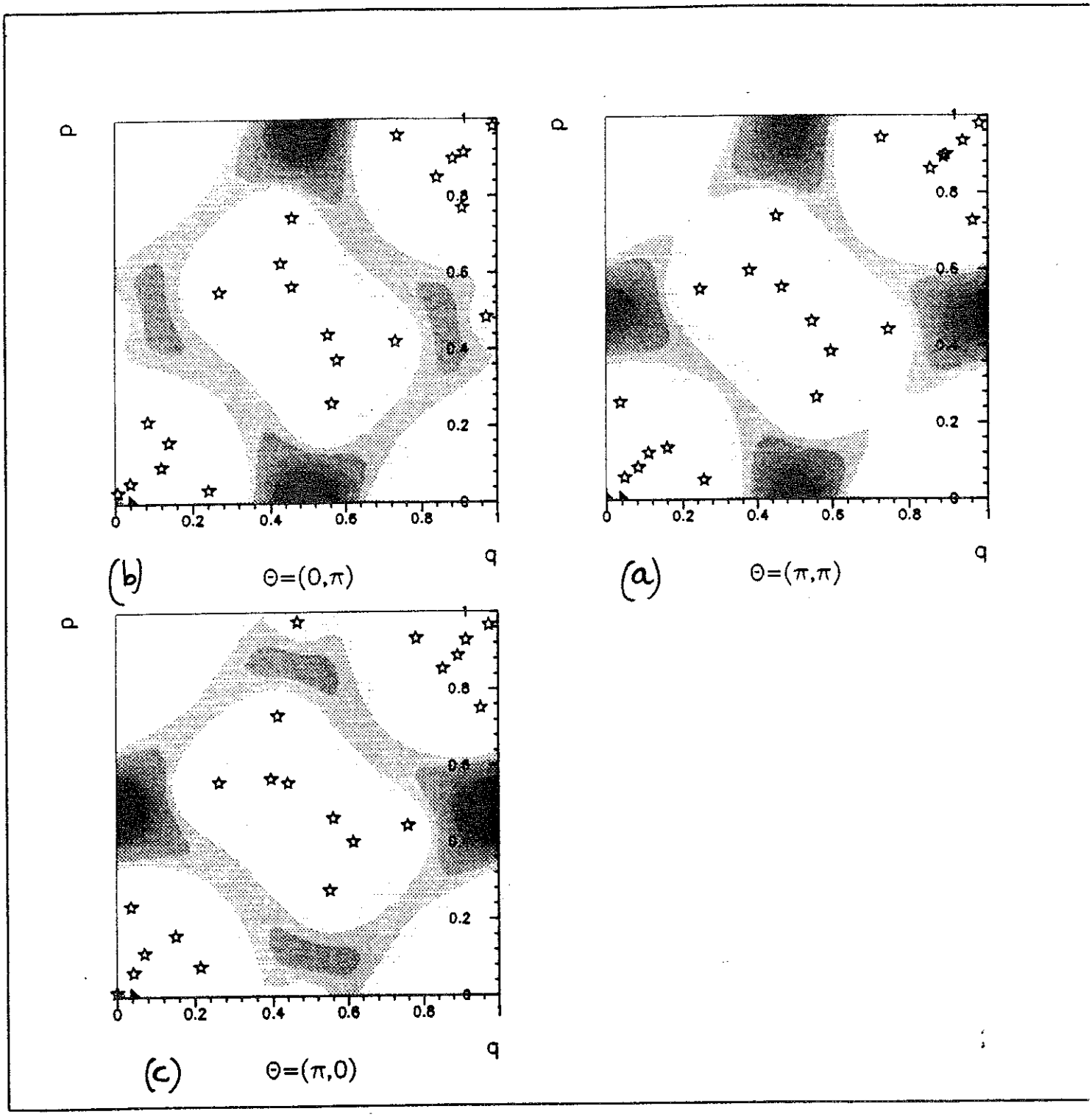

Figure 1

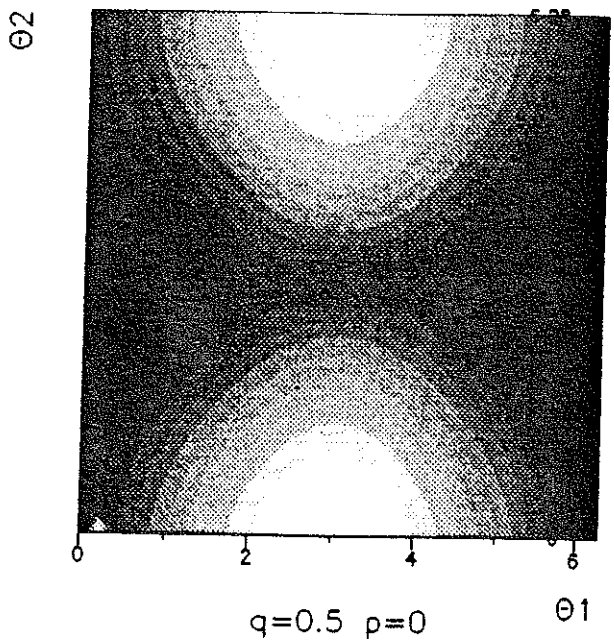

(a)

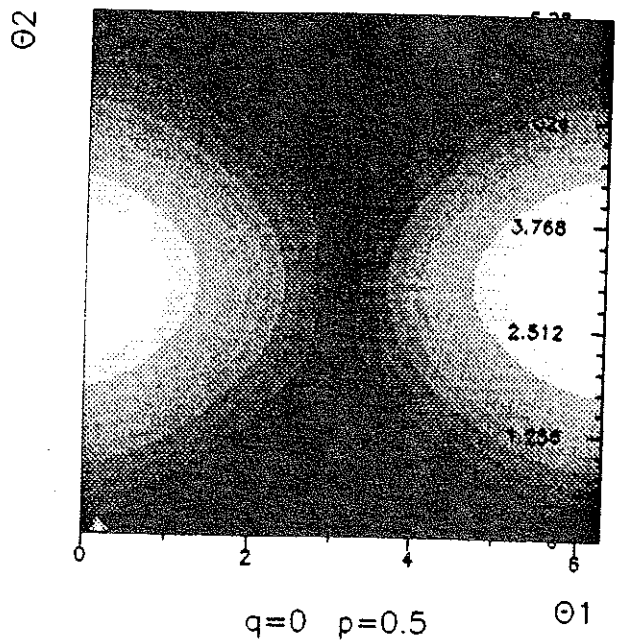

(b)

Figure 5

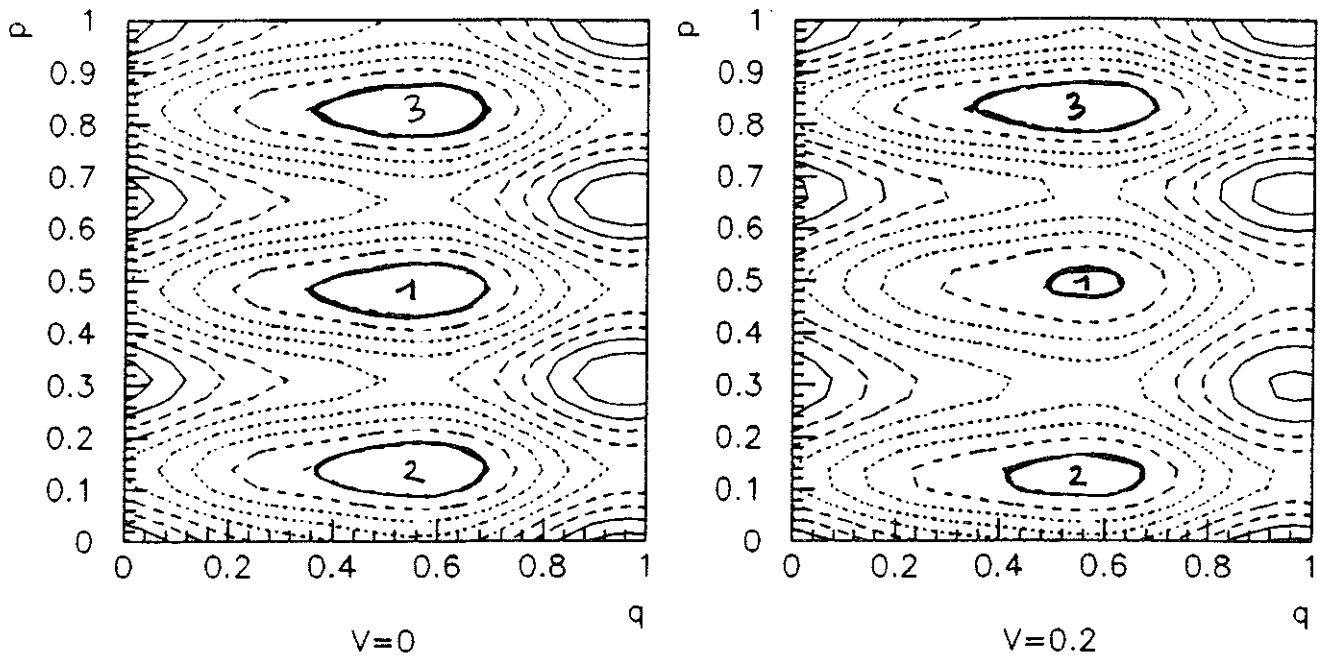

(a) (b)

Figure 6 (a)

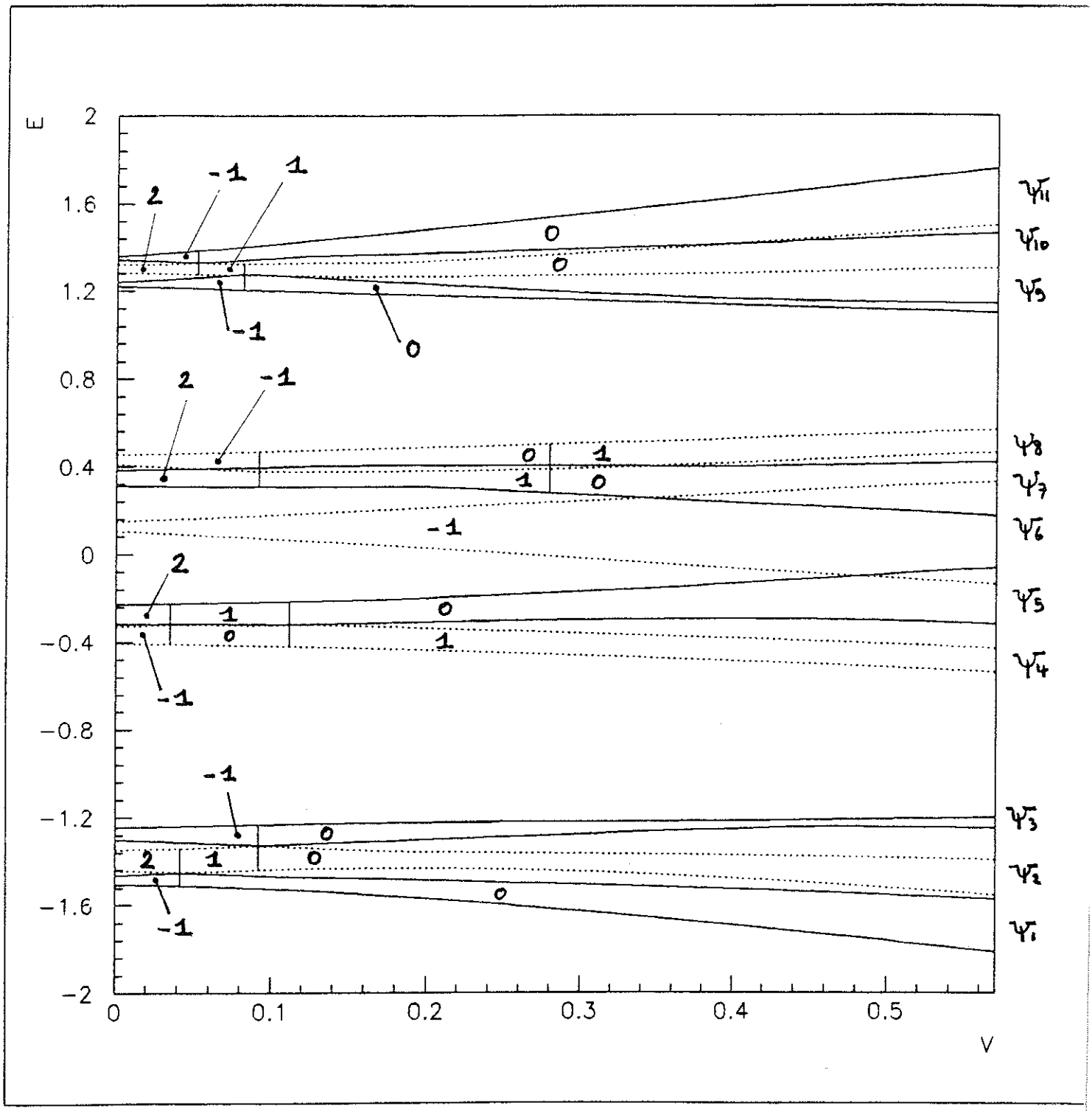
E
V
2
1.6
1.2
0.8
0.4
0
−0.4
−0.8
−1.2
−1.6
−2
0
0.1
0.2
0.3
0.4
0.5
ψ11
ψ10
ψ9
ψ8
ψ7
ψ6
ψ5
ψ4
ψ3
ψ2
ψ1

Figure 6 (b)

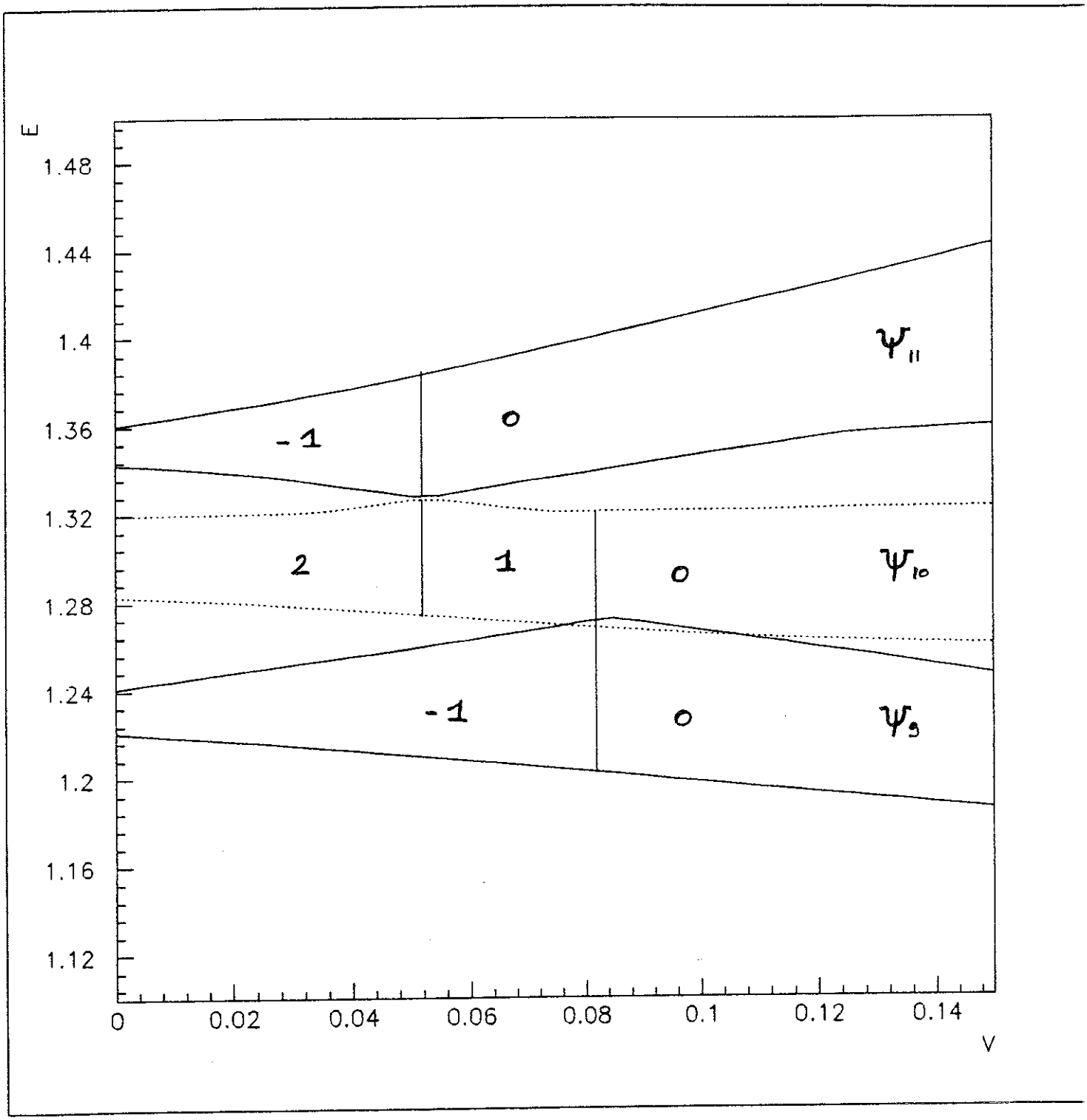
E
1.48
1.44
1.4
1.36
1.32
1.28
1.24
1.2
1.16
1.12
0
0.02
0.04
0.06
0.08
0.1
0.12
0.14
V
-1
0
2
1
0
-1
0
ψ_{11}
ψ_{10}
ψ_9

Figure 7

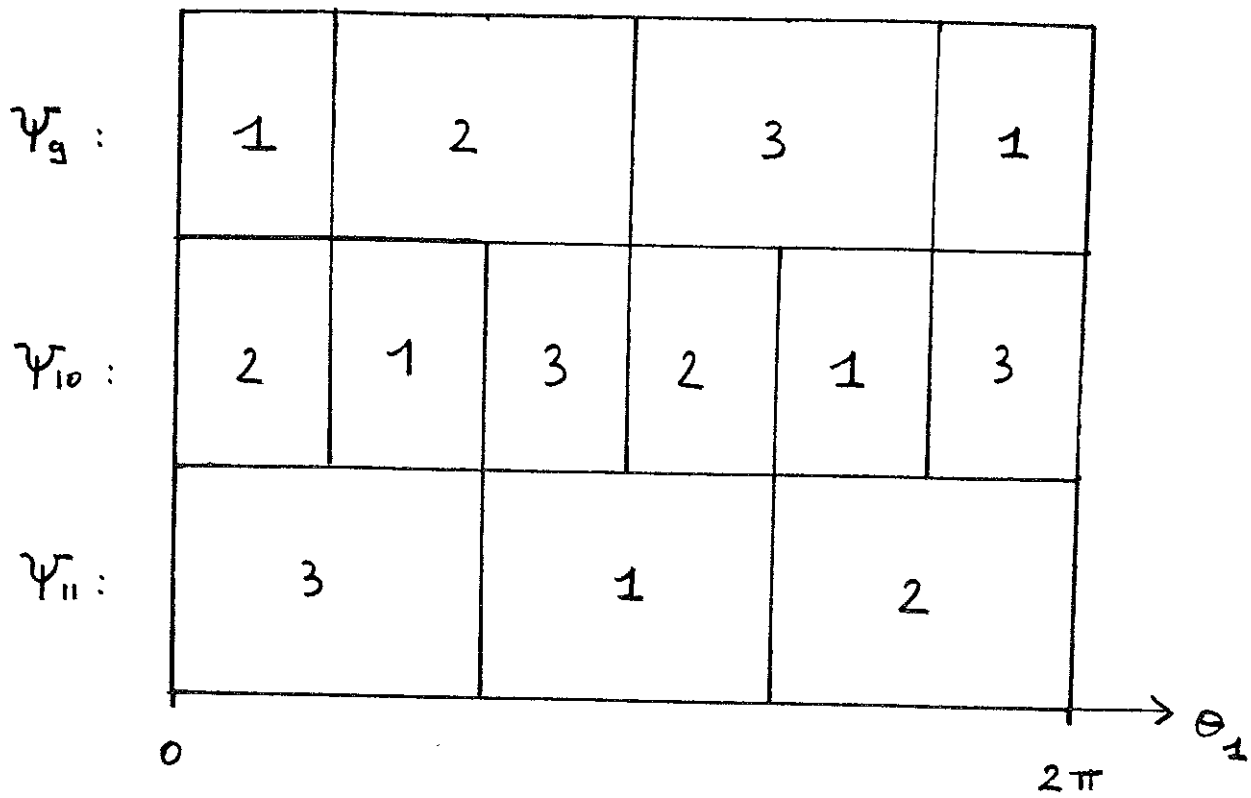

Figure 8

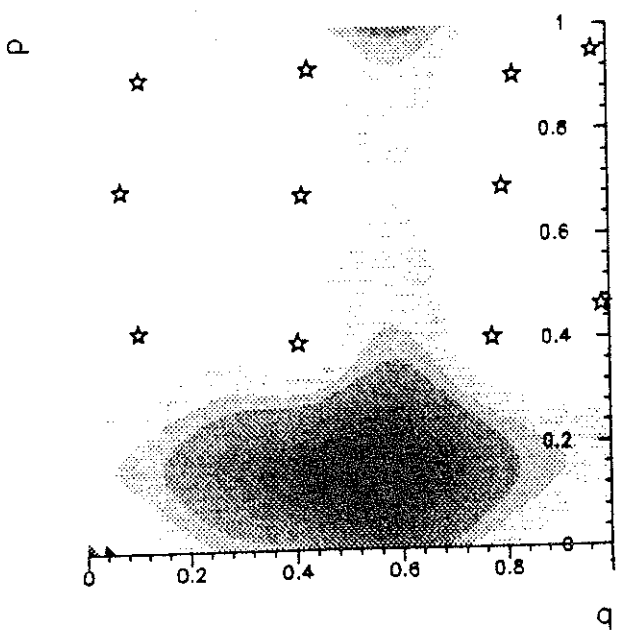

(a)

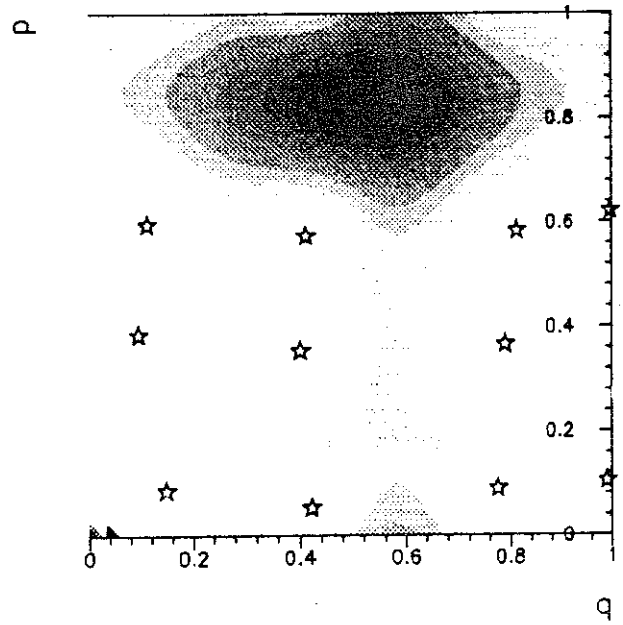

(b)

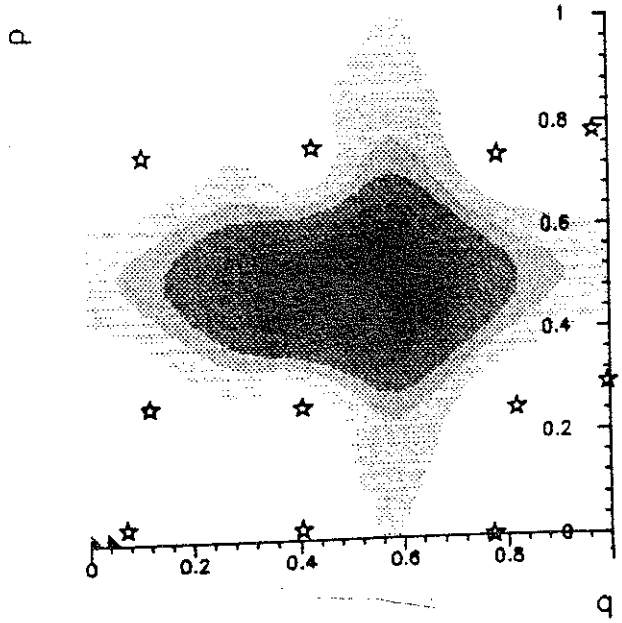

(c)

Figure 9

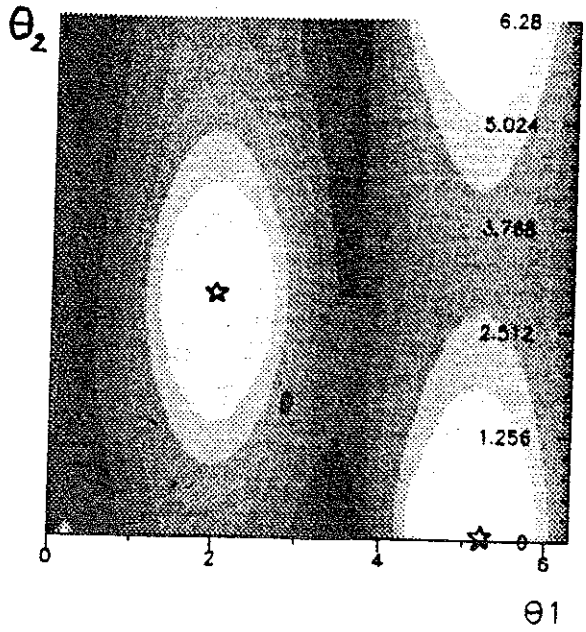
θ2
6.28
5.024
3.768
2.512
1.256
0
2
4
6
θ1

(a)

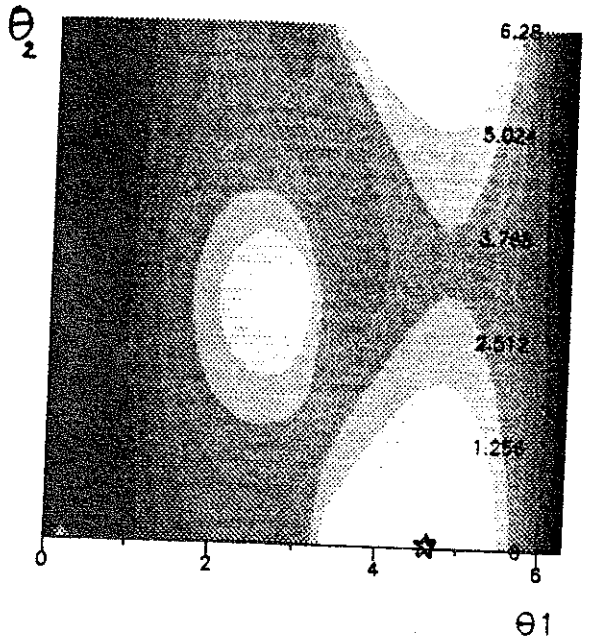
θ2
6.28
5.024
3.768
2.512
1.256
0
2
4
6
θ1

(b)

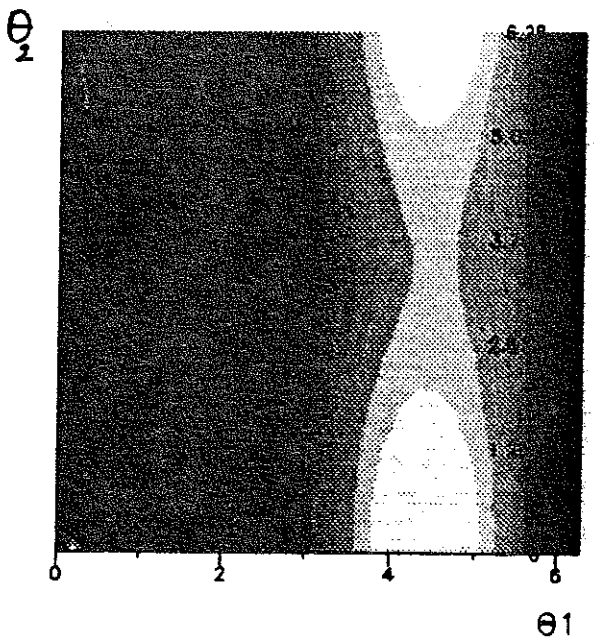
θ2
0
2
4
6
θ1

(c)

Figure 10

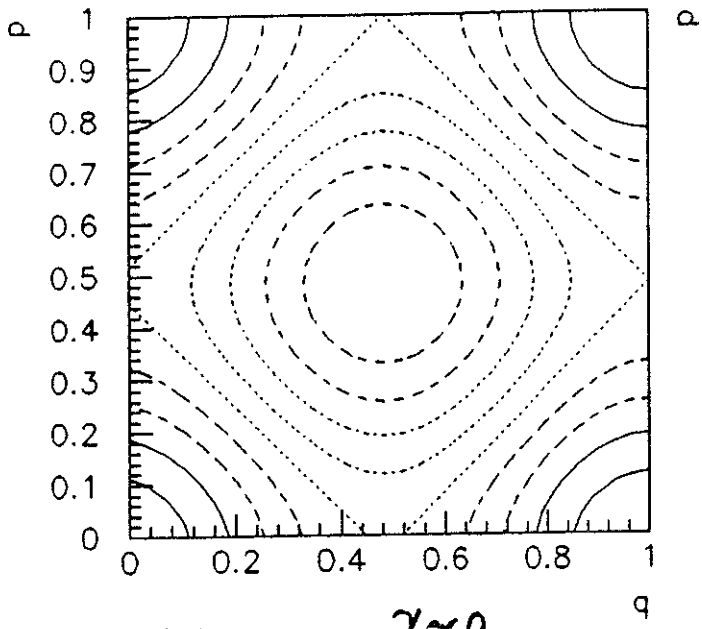

(a) $\gamma \approx 0$

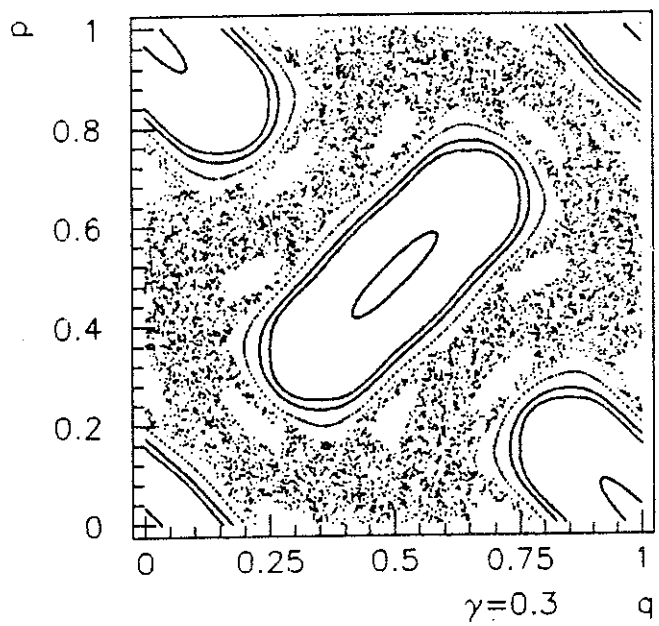

(b)

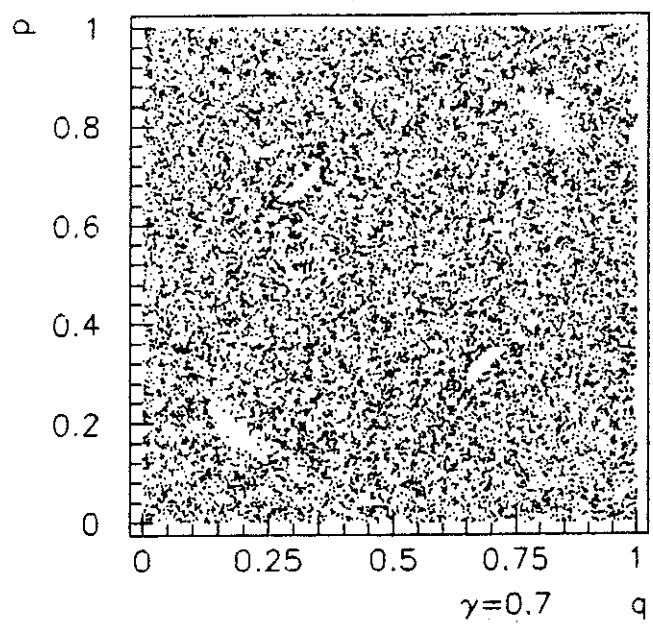

(c)

Figure 11

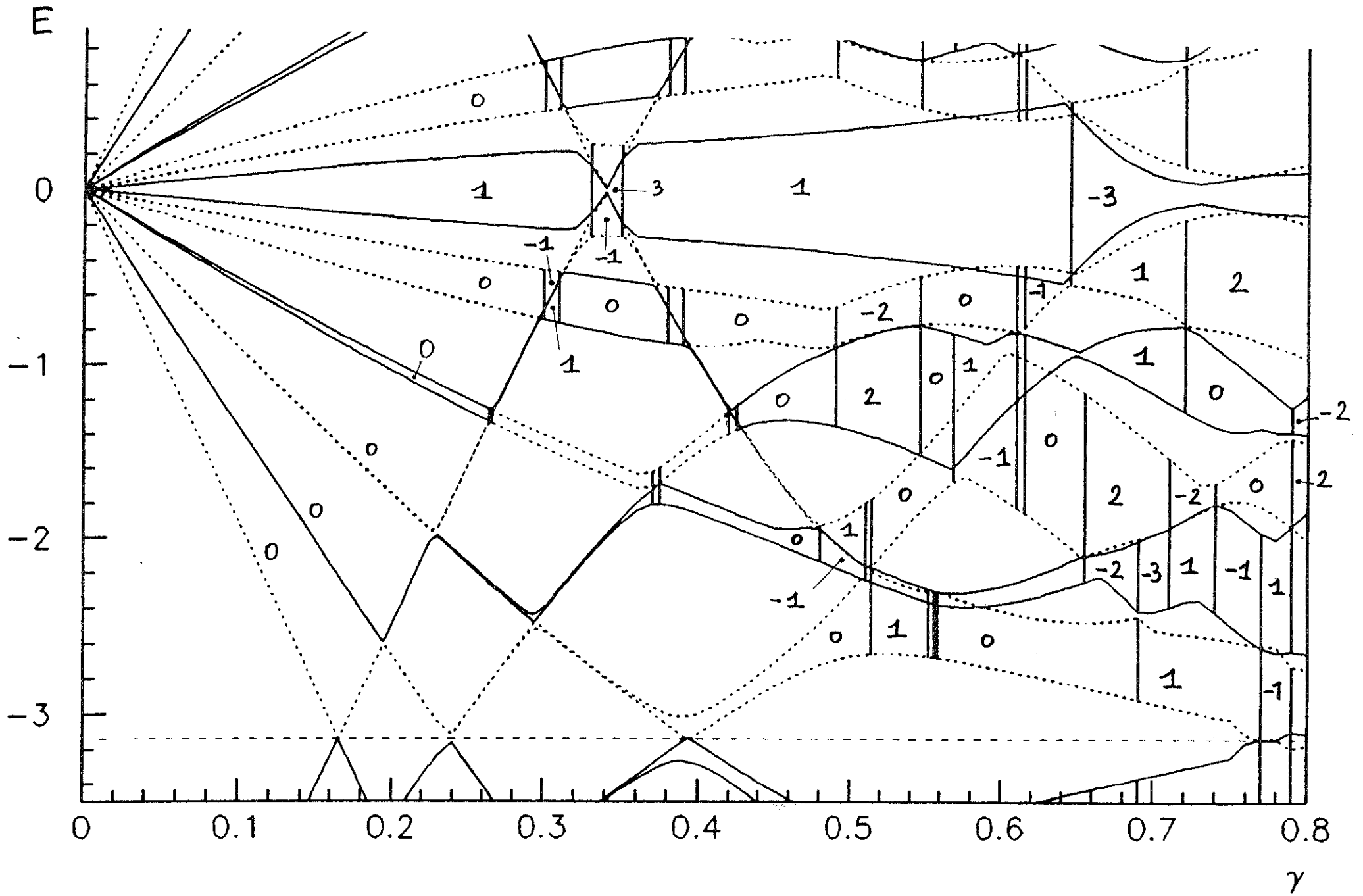

Figure 12 (a)

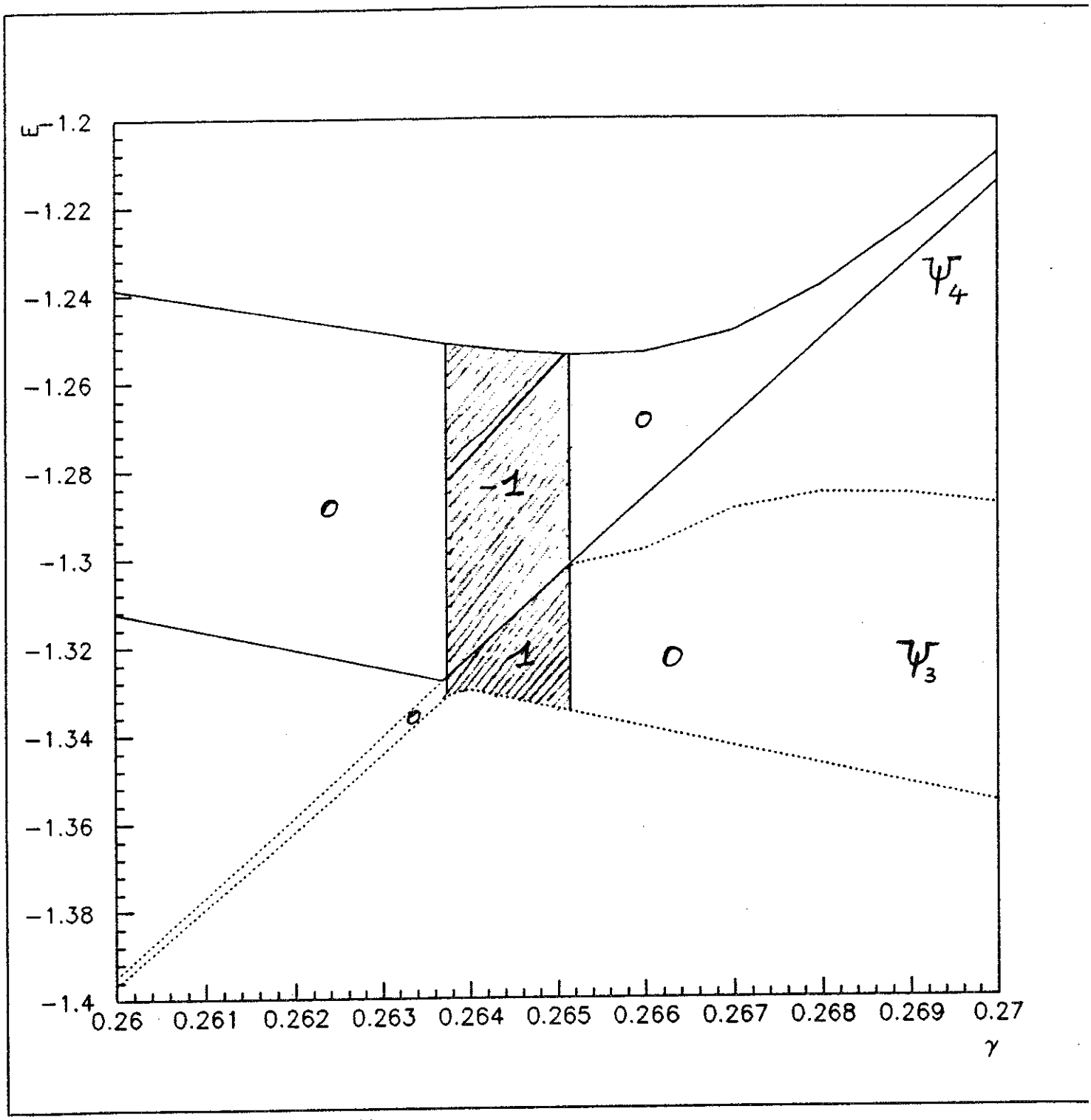
ω
-1.2
-1.22
-1.24
-1.26
-1.28
-1.3
-1.32
-1.34
-1.36
-1.38
-1.4
0.26
0.261
0.262
0.263
0.264
0.265
0.266
0.267
0.268
0.269
0.27
γ
ψ4
ψ3
0
-1
1

Figure 12 (b) (c) (d)

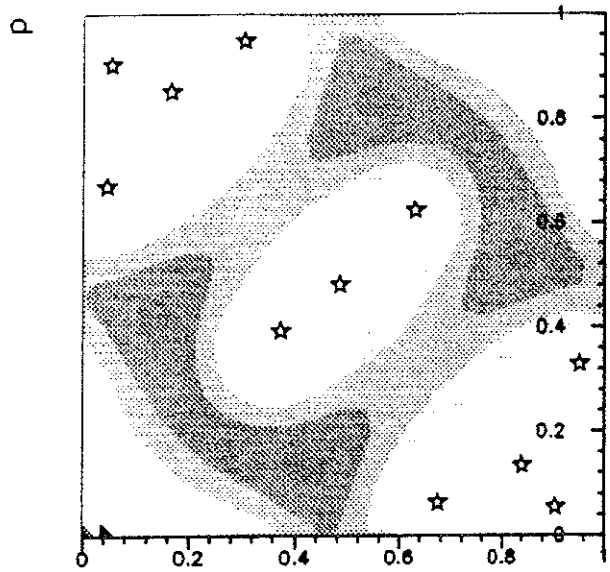

(b) $\Theta=(0,0)$

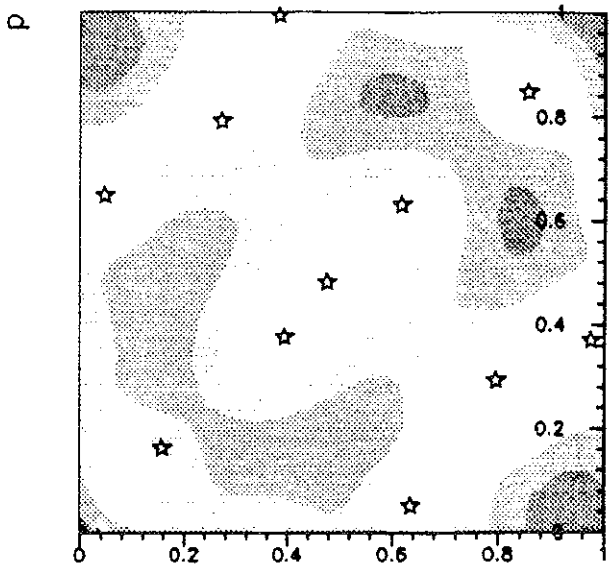

(c) $\Theta=(1,1)$

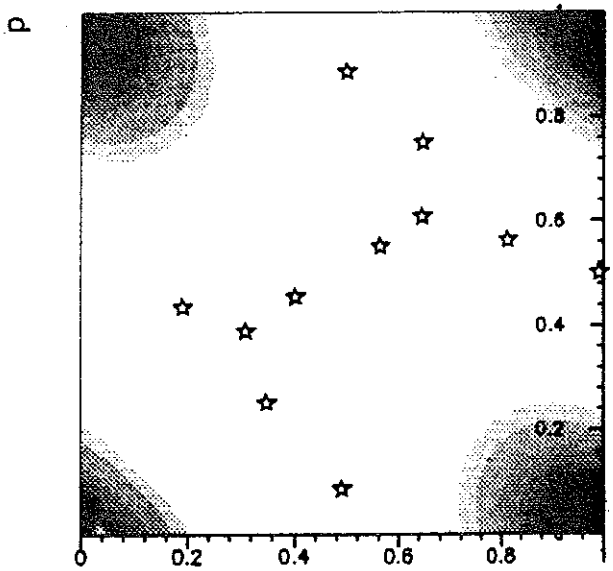

(d) $\Theta=(\pi,\pi)$